Chapter 5

Raman Study of the Crystalline-to-Amorphous State in Alpha-Decay–Damaged Materials

Ming Zhang

Additional information is available at the end of the chapter

http://dx.doi.org/10.5772/65910

Abstract

The stabilization and immobilization of high-level radioactive wastes in solid forms have become one of the most pressing industrial problems. Different crystalline mineral phases have been proposed as actinide-bearing crystalline hosts for waste materials. Self-radiation damage from alpha-decay of the incorporated actinides (such as U, Th) and other rare earth elements can lead to metamict state (amorphous state) and can affect the durability and long-term performance of these actinide-bearing phases. To investigate the impact of radiation on the nuclear waste forms and to obtain a better comprehension of the damage process and amorphization mechanism are important. The issues of interactions between high-energy particles and solids and radiation-induced structural modifications in crystalline-to-amorphous state are, in fact, an important and active area of fundamental researches. To study metamict state and metamictization is also important for geochemistry as the U-Pb isotope system is commonly used for age dating. Although radiation effect and naturally occurring radiation damage (the process is known as metamictization) have been the subject for many research investigations, there remain important and fundamental issues which need to be understood, for example, the structural changes at the atomic level caused by metamictization, the crystal structure of radiation-induced amorphous phases, solubility and diffusion of radioactive elements in damaged host phases, the effect of pressure and temperature on metamictization process and interaction of water and fluids with nuclear waste forms. Raman spectroscopy is found to be a very powerful tool for study and analysis of the damage effect and metamictization. This chapter describes and reviews recent Raman applications in zircon and titanite, which are proposed for nuclear waste forms. These applications are focused on radiation effect and structural damage process caused by alpha-decay process as well as recrystallization due to thermal annealing.

Keywords: Raman spectroscopy, radiation damage, metamictization, actinide, zircon, titanite

1. Introduction

Today, there are over 430 commercial nuclear power reactors in 31 countries which provide over 10% of the world electricity [1]. As a result, huge amounts of highly radioactive nuclear wastes are produced each year. One of the critical issues in nuclear energy industry is the safe disposal of nuclear wastes, especially high-level nuclear wastes (HLNW). The below are some minerals and synthetic materials proposed or developed as actinide-bearing crystalline hosts for waste materials [2–4]: zircon ($ZrSiO_4$), titanite ($CaTiSiO_5$), baddeleyite $(Zr,Hf,\ldots)O_2$, hafnon ($HfSiO_4$), perovskite $[(Ca,Gd,\ldots)(Al,Fe,Ti,\ldots)O_3]$, zirconolite [$CaZrTi_2O_7$ and $CaZrSi_2O_7$], apatite $[Ca_{10}(PO_4)_6(OH,F,Cl,B)_2]$, pyrochlore [$CaZrGd_2Ti_2O_7$, $Gd_2Zr_2O_7$, and $La_2Zr_2O_7$-$Nd_2Zr_2O_7$], monazite $[(La,Ce,\ldots)PO_4]$, and garnet $[(Ca,Fe,Gd,\ldots)_3\ (Al,Fe,Si,\ldots)_5O_{12}]$. Among them, zircon is one of the most studied and modeled minerals. Currently, pyrochlore has attracted attention because of its radiation damage resistance.

Self-radiation from alpha-decay of the incorporated actinides can lead to lattice damage resulting in structural change and transformation from crystalline state to an amorphous or aperiodic state, that is, metamict state (the process is known as metamictization) [5–7].

The effects of radiation damage on the structure of metamict minerals can be seen as systematic changes of its physical properties [8]: an increase in cell parameters and broadening of X-ray diffraction patterns [9–12]; a decrease in Raman and infrared intensities and dramatic band broadening [13, 14]; decreases in refractive index and birefringence [9, 15]; absorption of hydrous species [16–19]; an increase in fracture toughness [20]; a decrease in density [9, 10]; a variation of TEM diffraction patterns [10, 21, 22]; an increase of leach rate [23]; changes in bulk modulus and hardness [24]; a change of ^{29}Si NMR features [11, 25]; changes of diffuse X-ray scattering from single crystals [6]; occurrences of Huang type diffuse X-ray diffraction [26]; a change in EXAFS [27]; a variation of Mössbauer spectra [11, 28]; and a variation of positron annihilation lifetime [29]. Therefore, the durability and performance of these actinide-bearing phases can be altered by self-radiation damage from alpha-decay of the incorporated actinides. To gain better comprehension of the effect of radiation on crystal structure at the atomic level, the related damage process and damage mechanism are issues of critical importance.

Vibrational spectroscopy (Raman and infrared (IR) spectroscopy) is a very powerful tool in the analysis and study of structural variations related to medium- and short-range order [30]. Early analysis of alpha-decay damaged materials by Raman spectroscopy can be traced back to about two decades ago [31, 32]. The main advantages of vibrational spectroscopy (Raman and infrared spectroscopy) [30] are their fast response time (which can be in the range of ~10^{-12} s), short correlation length scale (which is in the order of a few unit cells), and good sensitivity to hydrous and hydroxyl species (e.g., H_2O and OH). In contrast to diffraction methods which are generally sensitive to periodicity of lattices and the crystallinity of a specimen, vibrational spectroscopy is mainly associated with the strength and length of interatomic bonds, as well as the atomic masses of the sample. Therefore, vibrational spectroscopy can give valuable information on phonon energy, bulk structure, chemical composition, and surface for not only crystalline materials, but also disordered phases. The method has, in fact, been widely applied in studying disordered and amorphous materials such as glasses.

http://dx.doi.org/10.5772/65910

This chapter illustrates recent applications of Raman spectroscopy in the study of radiation-damaged or metamict zircon and titanite. Being different from simple identification of damaged phases with Raman techniques, the investigations are focused on important issues such as: What happens at the atomic level during radiation damage and recrystallization? What are the possible structural modifications during metamictization? And whether decomposition into oxides is the final result of radiation damage. The experimental results provide a better understanding of the mechanism of radiation damage and the recrystallization processes.

2. Effects of alpha-decay radiation on Raman spectra of zircon and titanite

Zircon ($ZrSiO_4$) is a common accessory mineral in igneous rocks, in metamorphic rocks, and as detrital grains in sedimentary rocks. The work [33] has showed that zircon crystallizes to a tetragonal structure with space group D_{4h}^{19} or $I4_1/amd$ (with $Z = 4$), containing a chain of alternating, edge-sharing SiO_4 tetrahedra and ZrO_8 triangular dodecahedra extending parallel to the *c*-axis. Actinides such as U, Th and Pu can substitute Zr and locate in the Zr site. Because of their uranium and thorium content, some zircons undergo metamictization. Group theory predicts twelve Raman-active normal modes in zircon at $k = 0$: $2A_{1g} + 4B_{1g} + B_{2g} + 5E_g$ [34]. These Raman modes can be simply classified as internal modes and external modes. There are five ($2B_{1g} + 3E_g$) external modes and seven ($2A_{1g} + 2B_{1g} + B_{2g} + 2E_g$) internal modes. For Raman measurements of natural samples which are damaged by radiation of incorporated actinides, it is a good practice to use laser excitation with different wavelengths to ensure that spectral features recorded are due to phonon modes rather than features due to luminescence and impurities-related color centers (e.g., the work [8] used 514, 488, 457 and 632 nm lasers in its Raman measurement). Nine of the twelve predicted Raman modes can be seen in the most crystalline natural zircon (**Figure 1**). They are internal modes: 1008 cm^{-1} (B_{1g}, ν_3 stretching of SiO_4), 975 cm^{-1} (A_{1g}, ν_1 stretching), 439 cm^{-1} (A_{1g}, ν_2 bending), and 269 cm^{-1} (B_{2g}, ν_2 bending) and external modes: 393, 355, 225, 214 and 202 cm^{-1}. The other predicted Raman bands appear too weak to be observed in a common experimental arrangement.

The effect of alpha-decay radiation damage on the structure of zircon is evidenced by a decrease in band frequencies, a line broadening of Raman modes and a decrease in Raman intensity (**Figure 1**). Well-crystallized zircon samples have sharp and well-resolved Raman modes. With increasing alpha-decay radiation dose (the radiation dose of natural minerals is mainly related to sample's rock age and concentration of U and Th, and it can be calculated [9, 10]), the stretching modes of SiO_4 tetrahedra near 975 and 1008 cm^{-1} become weaker and broader, while the lower frequency modes become gradually weaker and could hardly be analyzed for high-dose cases. The broad Raman feature concurring near 950 cm^{-1} (the insert part in **Figure 1**) indicates the formation of amorphous phases in high-dose samples. The behavior of the band also suggests that SiO_4 tetrahedra remain in highly damaged zircon samples. As the 950 cm^{-1} feature is significantly away from the intense bands near 1008 cm^{-1} in terms of wavenumber, its appearance implies a new linkage of SiO_4 tetrahedra.

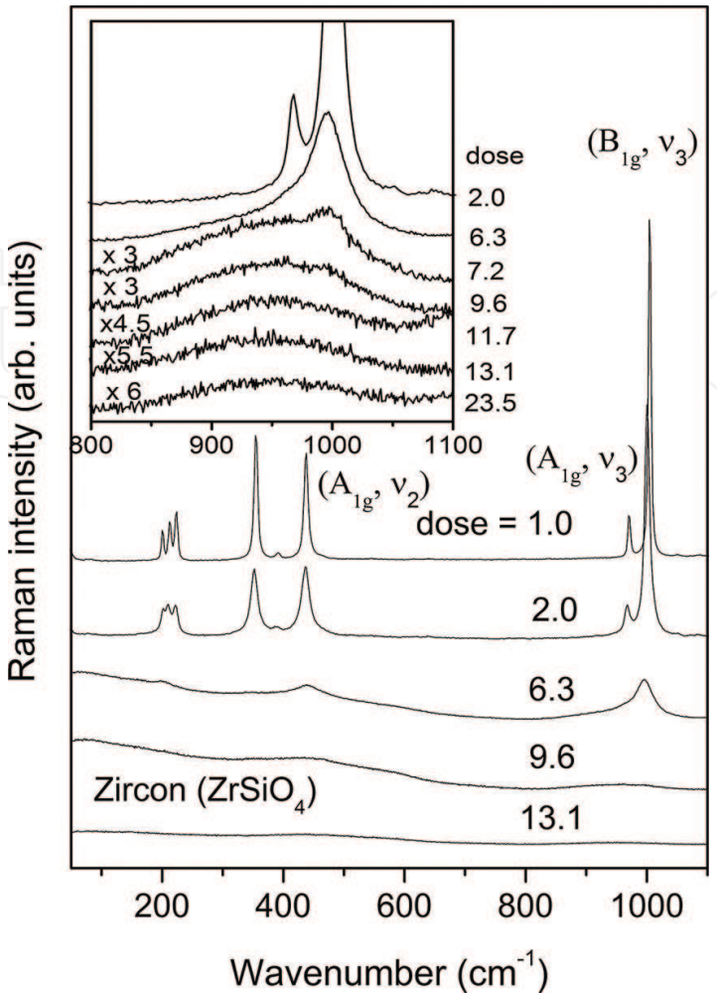

Figure 1. Micro-Raman spectra (with 488 nm excitation) of metamict zircon between 50 and 1100 cm^{-1} (Ref. [8], modified). The dosage is in the units of 10^{18} alpha-events g^{-1}.

The dose dependence of the frequency and full width at half maximum of the 1008 cm^{-1} stretching band of SiO_4 are shown in **Figure 2**. The data indicate that the Si-O bond strength exhibits a weakness, while the specific volume of the crystal increases, although radiation damage does not destroy SiO_4 and short-range ordering associated with the tetrahedral framework remains. The observation suggests that the increase in bond distances is probably depolarized by a rotation of the SiO_4 tetrahedra within the zircon structure. The data clearly show that the unit cell swelling in damaged zircon is associated with the SiO_4 tetrahedra which formed new linkage and play an important role in the zircon structure rather than isolated molecular complexes.

Raman band widths [full width at half maximum (FWHM)] and frequencies (especially those of the ν_3 band of SiO_4 near 1008 cm^{-1}) in zircon have been used for investigating the relationship between U-Pb isotopic discordance and metamictization [35–37]. More work is desirable to gain a better understanding of the behavior of this band during radiation damage and recrystallization, and the potential influence of chemical impurities on the band.

http://dx.doi.org/10.5772/65910

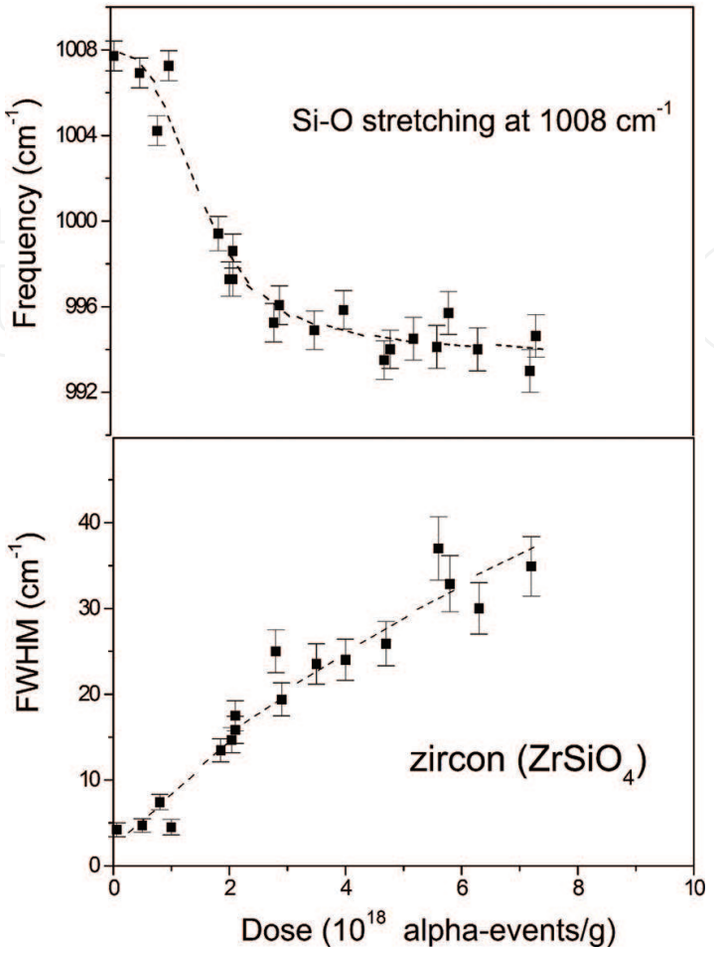

Figure 2. Phonon frequency and full width at half maximum (FWHM) of the ν_3 stretching band (B_{1g}) of SiO_4 in radiation-damaged zircon as a function of radiation dose (Ref. [8], modified). The lines are visual guides.

Another good example of Raman study of alpha-decay radiation damage is the application in metamict titanite. Titanite is a calcium titanium nesosilicate mineral, $CaTiSiO_5$. Taylor and Brown [38] synthesized pure titanite, and their X-ray data show that it is monoclinic (space group $P2_1/a$, $Z = 4$) with unit-cell parameters $a = 7.057$, $b = 8.707$, $c = 6.555$ Å, $\beta = 113.81°$. The crystal structure of $P2_1/a$ titanite phase contains chains of corner-sharing TiO_6 octahedra parallel along [1 0 0], which are cross-linked by edge-sharing CaO_7-polyhedra extending parallel to [1 0 1]. On heating, the $P2_1/a$ phase undergoes a phase transition to an $A2/a$ phase near 500 K [38]. The two phases have different optical active representations. For the $P2_1/a$ phase $\Gamma_{optic} = 24A_g + 24B_g + 23A_u + 22B_u$ (A_g and B_g are Raman-active, and A_u and B_u IR-active), whereas for the $A2/a$ phase $\Gamma_{optic} = 9A_g + 12B_g + 11A_u + 13B_u$ [39]. Therefore, the $P2_1/a$ phase is expected to have 48 Raman-active modes, whereas the $A2/a$ phase contains 21 Raman modes. Although pure synthetic titanite is in $P2_1/a$ symmetry, some well-crystalline natural titanite samples were surprisingly reported to be in the $A2/a$ structure [11]. This significant difference

in the total number of the Raman modes for the $P2_1/a$ and $A2/a$ phases is important and helpful for identifying the presence of the two phases [40].

Natural titanite occurs in igneous and metamorphic rock and incorporates a variety of impurity ions such as U, Th and other rare earth elements (REE). The structure of natural titanite is often metamict, as a result of self-radiation damage associated with the alpha-decay of the incorporated REEs. Raman spectra of crystalline or undamaged natural titanite (**Figure 3**) show spectral features similar to those of synthetic pure $P2_1/a$ titanite as reported previously [39]. The Raman work [41] suggested that anisotropy is preserved upon metamictization and that the structural state of highly metamict titanite should not be considered as quasi-amorphous. It was reported that the local structure of the amorphized regions contains a high degree of short-range order [42]. The effect of alpha-decay radiation on Raman spectrum of titanite is characterized by a dramatic decrease in intensity and line broadening (**Figure 3**).

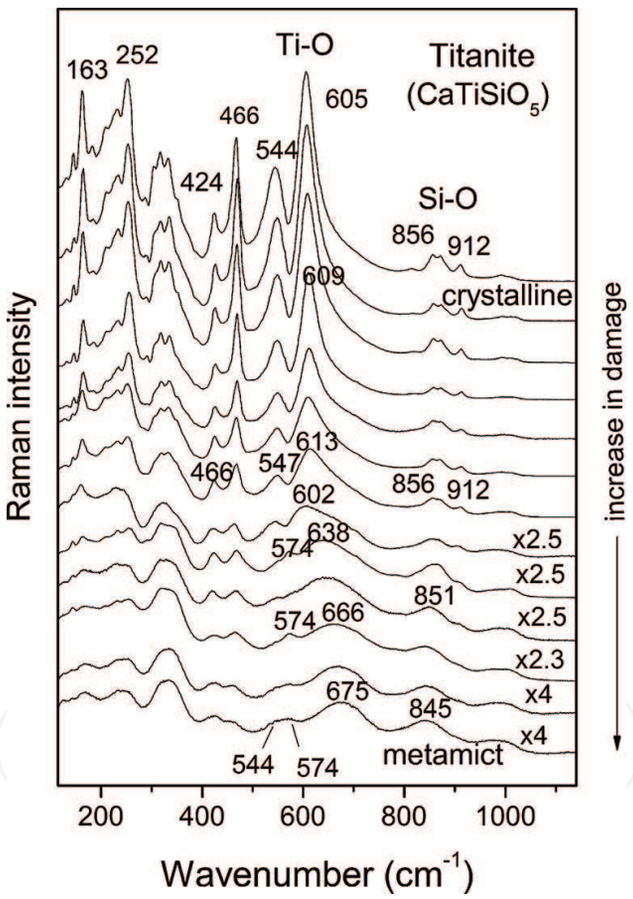

Figure 3. Raman spectra of fine powders of titanites ($CaTiSiO_5$) with different degrees of radiation damage (Ref. [40], modified). The top spectra are from well-crystallized samples, which show that the space group is the $P2_1/a$ symmetry [40]. Metamictization causes a loss of spectral details and a line broadening in the spectra of titanites. The Ti-O stretching band near 605 cm^{-1} shifts to a higher frequency, while a extra band near 574 cm^{-1} (which is due to the $A2/a$ phase) appears in partially damage samples. A relatively intense band is recorded near 675 cm^{-1} with a FWHM of about 80 cm^{-1} in heavily damaged titanite (in the bottom of the plot). The large FWFM indicates that this feature is related to radiation-induced disordered or amorphous phase. Crystalline titanites have the bands near 858 and 912 cm^{-1}, which are due to stretching vibrations of SiO_4 tetrahedra. These bands shift to lower frequencies in intermediately damaged samples and appear as a broad feature near 845 cm^{-1} in heavily damage samples (bottom).

http://dx.doi.org/10.5772/65910

The intense Ti-O band near 605 cm^{-1} shows the largest intensity decrease, indicating radiation effect on the TiO_6 octahedra. This change is consistent with the behavior of the infrared-active Ti-O stretching mode near 670 cm^{-1}, which is mostly affected by radiation damage and shifts to 710 cm^{-1} in heavily damaged titanite [43]. A Raman work on metamict titanite [44] proposed that radiation-induced periodic faults in the crystalline matrix of metamict titanite are related to the disturbance of SiO_4-TiO_6-SiO_4-TiO_6 rings comprising TiO_6 octahedra from different chains, whereas the radiation-induced amorphization is associated with the partial change of Ti coordination from octahedral to pyramidal and/or tetrahedral, which in turn violates the Ti-O-Ti intrachain linkages. In addition to these changes, radiation damage in titanite leads to the appearance of extra Raman signals (e.g., 574 cm^{-1}) in intermediately damaged samples (**Figure 3**). This behavior is not seen in metamict zircon. These additional phonon modes in these partially metamict titanite samples are, in fact, characteristic Raman bands of the *A*2/*a* phase [40]. The results indicate that as a result of the radiation, the $P2_1/a$ titanite first transforms to the *A*2/*a* structure, and then, with further radiation, the *A*2/*a* phase becomes an amorphous phase. Beirau et al. [45] reported in situ high-temperature Raman data of radiation-damaged titanite, and they found a structural anomaly near 500 K in partially metamict titanite, which was attributed to the $P2_1/a$-*A*2/*a* transition. These above findings explained why some of natural crystalline titanites were found to appear the *A*2/*a* structure [11], rather than the $P2_1/a$ phase. This could be due to the fact that natural titanite crystals commonly experienced radiation damage, which resulted in an alteration of the $P2_1/a$ crystal structure [40].

3. Issue of possible decomposition in radiation-damaged zircon

In the study of radiation effect and metamict state, what happens at the atomic level is an unclear and important question. Researchers have focused on issues such as possible changes in the coordination number of Zr [27], radiation-induced disordering rather than amorphization [31], damage-related distorted and disoriented isolated silica tetrahedra [16], the fraction of amorphized phase [14, 46], as well as whether metamictization leads to phase separation or damaged minerals decompose into their oxides, and what is the structural state of the decomposed phases [47, 48]. This issue of radiation-induced decomposition was, in fact, debated over decades [30]. Based on infrared data on metamict zircon, a two-stage damage process was proposed [49]. It was suggested that the first stage produces, throughout the lattice, highly stressed and expanded zircon with distorted SiO_4 tetrahedra, while the second stage was suggested to result in the decomposition of $ZrSiO_4$ to ZrO_2 and SiO_2, probably together with some aperiodic $ZrSiO_4$ [49]. However, the decomposition of damaged zircon was often reported in zircon samples only annealed experimentally at high temperatures, in which the decomposition commonly leads to different polymorphs of ZrO_2 and glassy silica. Monoclinic ZrO_2 was found in heavily damaged samples heated to 1373 K [50]. In a high-temperature study, Vance and Anderson [15] observed cubic and tetragonal ZrO_2 at 1073 and 1373 K, respectively. It was reported that highly metamict zircon contained randomly orientated ZrO_2 when annealed at 1173 K, and further annealing at 1523 K resulted in monoclinic ZrO_2, as well as a silica glass phase [51]. Ellsworth et al. [52] suggested that decomposition of metamict zircon into ZrO_2 and glassy SiO_2 could be one possible path for recrystallization. In contrast,

a high-temperature neutron work by [53] suggested that zircon decomposes into crystalline β-cristobalite (rather than silica glass) and tetragonal ZrO_2. An X-ray powder diffraction study at high temperatures reported the appearance of pseudo-cubic ZrO_2 [54]. Meldrum et al. [55] observed a decomposition of zircon into tetragonal ZrO_2 when irradiating zircon with heavy ions at around 950 K. As discussed by different works [56, 57], some of these previous works based on X-ray diffraction measurements might have experienced difficulties in the determination of cubic and tetragonal ZrO_2.

Vibrational (Raman and infrared) spectroscopy is a good analytical tool for resolving these problems related to decomposition of $ZrSiO_4$ into ZrO_2 and SiO_2, as pointed out by Ref. [30], because Raman and infrared spectra of zirconia (ZrO_2) have been well studied previously and also because vibrational spectroscopy has short length scales. ZrO_2 has three common polymorphs at different temperatures. The room-temperature phase is monoclinic, while the tetragonal and cubic phases occur at high temperatures [58]. The theoretical calculations [59, 60] have given the optical phonon modes (for zero wave vector) for each polymorph of zirconia ZrO_2. The monoclinic ZrO_2 has space group C_{2h}^5 /$P2_1/c$ and $Z = 4$, and it has eighteen Raman modes and fifteen infrared modes [$9A_g(R) + 9B_g(R) + 8A_u$ (IR) + $7B_u$(IR)] (R indicating Raman-active and IR indicating infrared-active). In tetragonal ZrO_2 (with space group D_{4h}^{15} /$P4_2/nmc$ and $Z = 2$), the phase has six Raman modes and three infrared modes [$A_{1g}(R) + 2B_{1g}(R) + 3E_g(R) + A_{2u}(IR) + 2E_u(IR)$]. For cubic ZrO_2 (with space group O_h^5 /$Fm3m$ and $Z = 1$), its vibrational spectra have only one Raman and one infrared modes [$F_{2g}(R) + F_{1u}(IR)$].

The data in **Figure 1** indicate that it is apparent that there is a lack of signals of ZrO_2 in highly damaged zircons. This shows that ZrO_2 and SiO_2 are not the final products of metamictization in zircon. Results from infrared spectroscopy of radiation-damaged zircon [14, 47] also support this observation. As mentioned early, although decomposed zircons were commonly reported in lab-treated samples, tetragonal ZrO_2 was recorded in only one natural sample [8], with an unknown thermal history, among a large number of natural zircon samples with different degrees of damage analyzed in Refs. [14, 47, 48]. In order to explore and examine high-temperature behavior of damaged zircon and the possible causes for decomposition in zircon, systematic works were carried out by different groups [47, 36, 61, 62]. These works show that thermal annealing of heavily damaged zircon at high-temperature experiments may lead to the decomposition of metamict zircon into tetragonal ZrO_2 and glassy SiO_2 at 1200 K, and upon further heating tetragonal ZrO_2 transforms to monoclinic ZrO_2 near 1400 K. Undamaged and weakly damaged zircons are less likely to show decomposition during high-temperature annealing. It was reported that the decomposition-induced silica tended to evaporate on further heating [61, 63]. As naturally damaged samples might experience high-temperature processes, some reported decomposed metamict zircon could be due to natural thermal annealing prior to experiments. In contrast to high-temperature annealing, the presence of ZrO_2 in some natural zircons might be due to the reaction of fluids with metamict zircons, because radiation damage may alternate the chemical stability of zircon. The observation of ZrO_2 in dissolution experiments was reported in highly damaged zircon samples [64]. Raman data of hydrothermally leached metamict zircon [65] showed the formation of

http://dx.doi.org/10.5772/65910

monoclinic ZrO_2. In general, the decomposition of zircon into ZrO_2 and SiO_2 is related to radiation-damaged zircons. Their crystal lattice is heavily damaged and has more defects. As a result, the durability of these heavily damaged samples is expected to be affected, and they are vulnerable to the impact of external physical and chemical conditions (e.g., water, solutions, high temperature, and even high pressure).

Raman data of metamict titanite (**Figure 3**) also show there is a lack of formation of oxides in highly damaged samples [40]. The findings are supported by X-ray measurements and TEM [11] and infrared data [43]. The observation further shows that phase decomposition into oxides is not the final state of alpha-decay damage in these materials, and the materials are safe to be used as nuclear waste forms. It has been found that decomposition of radiation-damaged zircon is commonly related to high-temperature heating (see a below section).

4. Metamict state *versus* glass state of $CaTiSiO_5$ and $ZrSiO_4$

One of the interesting issues related to radiation damage and metamictization is the similarities or differences between the amorphous phases produced by alpha-decay radiation damage and those produced through thermally quenched glass melts. Previous studies [47] have led to unanswered questions and concerns: for example, What is the relationship between the structural characteristics of disordered materials and the type of irradiation or physical process used to produce them?

As a type of disordered or amorphous materials, metamict minerals were commonly considered as "glass-like" materials in early studies on naturally occurring radiation effect and metamictization, and the metamict state was referred as a glassy state, which is somehow similar to that obtained by rapid quenching of high-temperature melts [30]. With experimental data gathering, evidences have emerged that indicate their important differences between the aperiodic states. The dispersion depends on the physical processes, which produce the amorphous states. Vibrational spectroscopy (Raman and infrared) is very useful to study this issue because of its sensitivity to local structures.

Raman data of metamict titanite ($CaTiSiO_5$) and its glass analogue (with the same chemical compositions) produced by quenching melts show that the two types of materials have different vibrational features (especially in the Ti-O and Si-O stretching regions) (**Figure 4**) [40], although they both are almost amorphous in terms of electron microscopy and X-ray diffraction analysis. The $CaTiSiO_5$ glasses produced from melts show a Si-O stretching band near 827 cm^{-1}, while metamict titanite has a relatively weak band in a higher wavenumber, 844 cm^{-1}. What is more, the quenched melts of $CaTiSiO_5$ have a relatively strong band peaked near 709 cm^{-1}, but this feature is almost absent in metamict titanite. The Raman observations are supported by the results for the same samples analyzed by infrared reflection and absorption spectroscopy [43]. These results suggest structural differences associated with Ti-O and Si-O bonds in the glasses and metamict phases. Interestingly, the glassy and metamict titanites also exhibit some similarities in a couple of band positions in the far infrared region (below 450 cm^{-1}). For example, they both have bands around 170, 330 and 430 cm^{-1}.

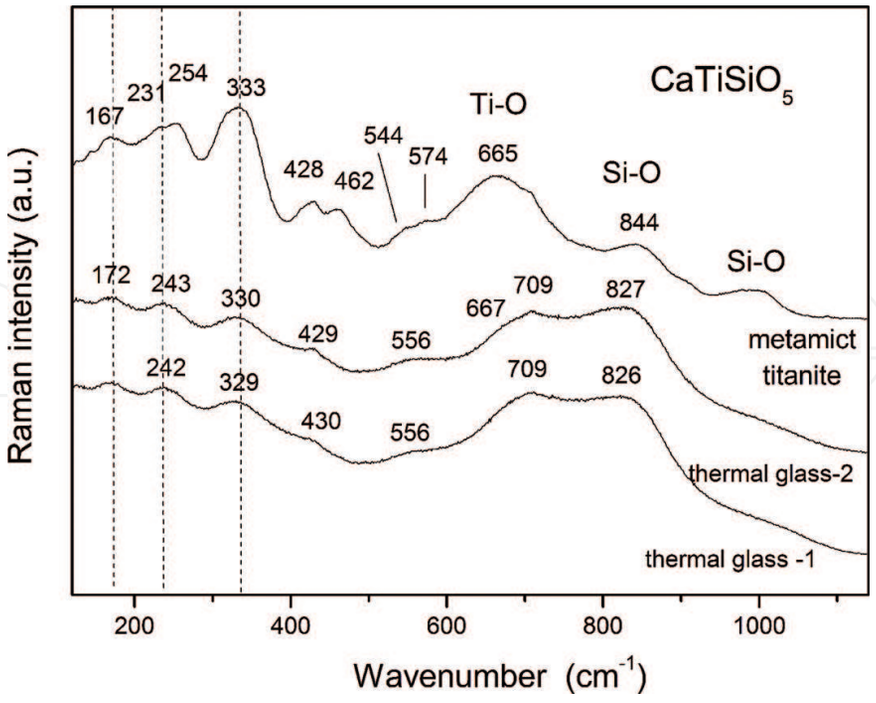

Figure 4. $CaTiSiO_5$ glasses produced by quenching titanite melts (thermal glass-1 and thermal glass-2 are prepared by quenching $CaTiSiO_5$ melts) show overall spectra patterns different from those of metamict titanite, especially in the region of 600 and 1100 cm^{-1} [Ref, [40], modified). This indicates the spectral dispersion related to Si-O and Ti-O vibrations in the two types of disordered materials. However, the two materials exhibit some local maximums with similar or close peak positions (indicated by dash lines) in the far infrared region (100 and 500 cm^{-1}).

Zircon has a high melting temperature (above 2700–2800 K), and crystalline ZrO_2 and a liquid of SiO_2 may coexist for a composition of $ZrSiO_4$ at a temperature region of ~1960 K and ~2670 K [66]. It is difficult to quench zircon melts without decomposition into ZrO_2 and SiO_2; however, glass-like zircon ($ZrSiO_4$) has been recorded with Raman spectroscopy in laser-treated zircon in a study with laser melting, near the boundaries between the unmolten and molten regions (where a relatively large temperature gradient could exist) [67]. The large temperature gradient is expected to increase the quench rate and facilitate a "freeze" of the local configuration of the $ZrSiO_4$ melts before the decomposition takes place. These experimental results indicate that the metamict state is different from the glassy state obtained by quenching melts. Apparently, the processes and structural states associated with metamictization and irradiation amorphization are more complex than those in common thermal glasses. The formation of the metamict state involves not only amorphization, but also defect accumulation caused by alpha-particle damage and further radiation or irradiation may lead to damage as well as recrystallization.

So far, although the issue remains under debates, there have been substantial evidences indicating characteristic discrepancies between two types of amorphous states (metamict and glass states) [68], for example: (i) the two types of materials commonly have spectral and structural discrepancies [40, 43, 69, 70]; (ii) high-energy heavy ion irradiation may lead to significant modifications in local structures of glasses [71–74]; (iii) upon heating, radiation-damaged minerals tend to recrystallize epitaxially and recover to their original

http://dx.doi.org/10.5772/65910

cryptographic orientations [48, 51, 75], while during high-temperature treatments, glasses commonly undergo a glass transition; and (iv) for common glasses, their glass transition temperatures are roughly defined, while various responses at different temperatures are seen in metamict minerals. For example, radiation-induced defects in metamict zircon may be annealed or healed at temperatures as low as 600 K accompanied by changes in the oxidation state of U ions; partial decomposition of $ZrSiO_4$ into SiO_2 and SiO_2 in heavily damaged zircon may take place at 1050 K; diffusion and conversions of hydrogen-related species together with dehydroxylation may occur between 1200 and 1600 K (e.g., [16, 18, 52, 76, 77], see for the transition point [6]).

5. Effect of thermal annealing on metamict zircon and titanite

Thermal annealing of metamict minerals at high temperatures is commonly used in studies of radiation-damaged minerals [30]. Its aims are to restore the original crystal structure for the purpose of studying recrystallization temperature, activation energy, types of radiation-induced local defects and phase identification, and to obtain a good comprehension of the recrystallization process and mechanism. Extensive studies were carried out to investigate changes at the atomic level in metamict materials during high-temperature annealing [10, 15, 36, 40, 44, 47, 48, 50, 52, 54, 55, 65, 75, 78–81]. However, controversies remain regarding the recrystallization path and activation energy.

Thermal annealing results in recrystallization of metamict zircon (**Figure 5**). The effect of annealing temperature on the structural recovery of damaged zircon can be clearly seen in the frequency and FWHM of the ν_3 Si-O stretching (B_{1g}) as a function of temperature (**Figure 6**). With increasing annealing temperature, the frequency of this mode shows, systematically, a large increase in the region between 800 and 1050 K and a weaker increase with temperature above 1050 K. This is due to the healing of the defective lattice and the recrystallization of remaining crystalline domains. Highly damaged zircon tends to decompose into tetragonal ZrO_2 and SiO_2 near 1100 K, and the transformation of tetragonal ZrO_2 into monoclinic ZrO_2 is reported at higher temperatures [47]. The findings may explain the cause of some previously reported ZrO_2 and SiO_2 in natural zircon, which likely experienced natural heating processes.

Spectroscopic data [47, 48, 61] revealed different recrystallization processes between partially and heavily damaged zircons, that is, the recrystallization process depends on the cumulative radiation dose (**Figure 5**, **6a** and **6b**). Being similar to metamict zircon [47], the thermal response of the damaged titanite ($CaTiSiO_5$) is affected by their initial degrees of damage, that is, at the same treatment conditions, weakly or partially damaged samples are more likely to recover to crystalline titanite as compared with highly metamict samples [40]. Intermediately and heavily damaged titanite samples show a recovery of Ti-O and Si-O bands after annealing at 1300–1400 K, and these recovered crystals are consistent with the $P2_1/a$ symmetry, although in terms of band widths, they are far from a fully recovering [40]. Similar results were reported by the work of another group [44] who thermally treated a metamict titanite sample, which has an accumulated radiation dose of 1.2×10^{18} alpha-event/g by multistep annealing up to 1173 K, and found it was insufficient to recover the crystalline structure of the studied sample.

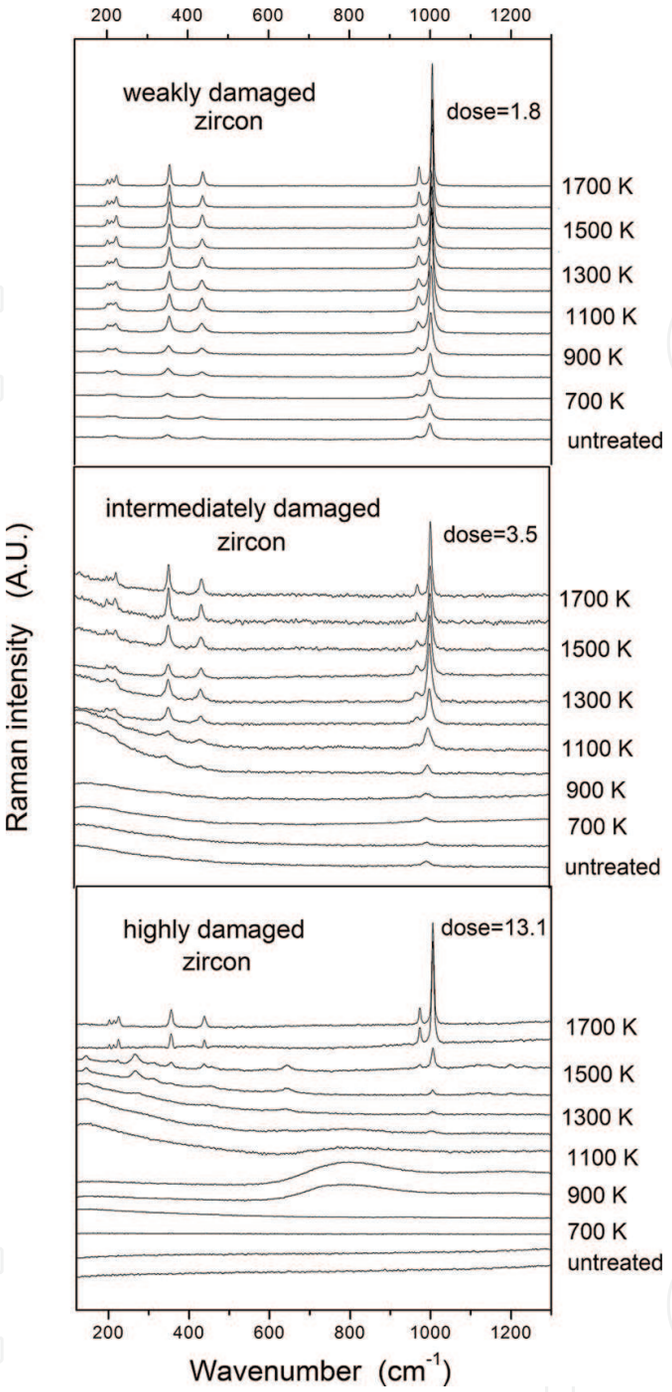

Figure 5. Raman spectra recorded from weakly metamict (dose = 1.8×10^{18} alpha-events g^{-1}), intermediately metamict (dose = 3.5) and highly metamict zircon (dose = 13.1) thermally treated in N_2 up to 1700 K and then punched (Ref. [47], modified).

The failure of a full recovery from the damage in thermally treated metamict titanite is also revealed by infrared spectroscopy [43]; however, the physics behind this remain unclear.

The thermally induced structural recovery and recrystallization of metamict zircon and titanite is also characterized a recovery of the anisotropy of the sample, which is restored

http://dx.doi.org/10.5772/65910

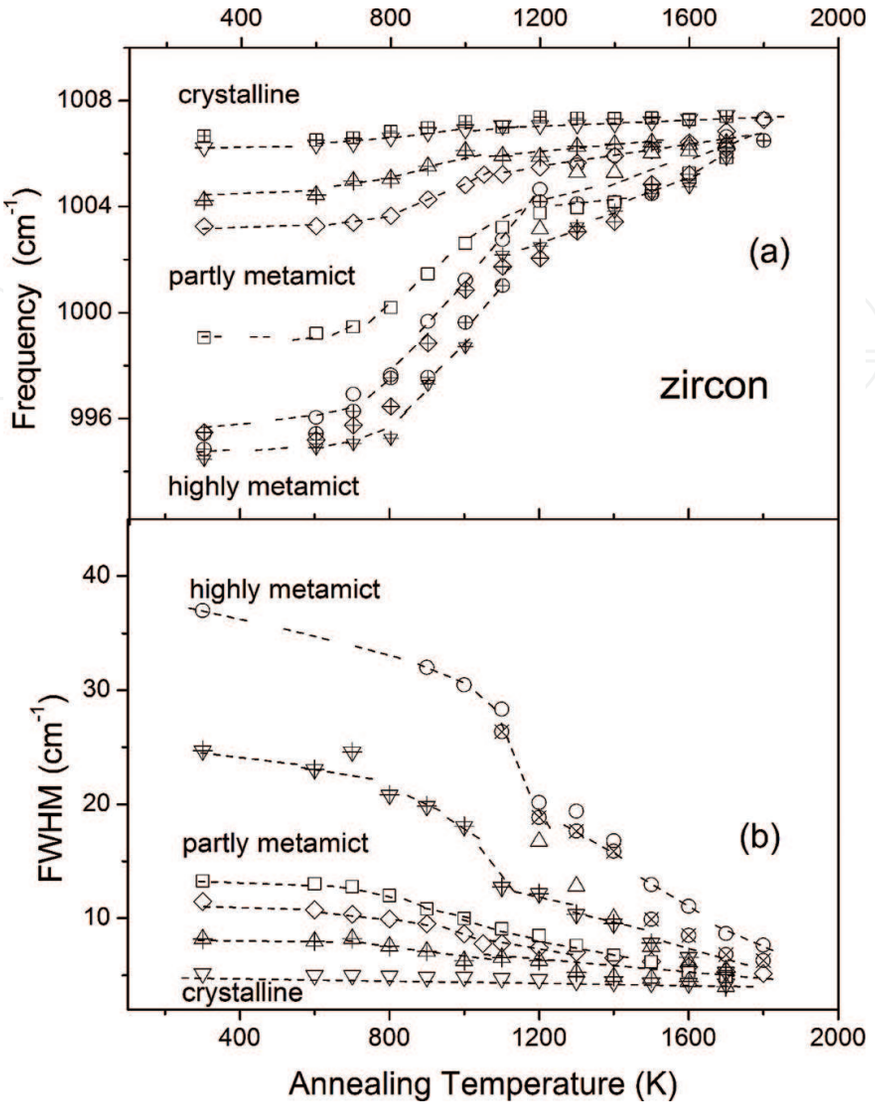

Figure 6. Phonon frequency and FWHM of the Raman ν_3 Si-O stretching (B_{1g}) in zircon ($ZrSiO_4$) with different degrees of damage as a function of annealing temperature (Ref. [47], modified with unpublished data).

during annealing, as evidenced by the recovery of orientational dependence of IR (as well as Raman) spectra along with the original crystallographic orientations as shown in **Figure 7**, which indicates an epitaxial recrystallization. This behavior indicates that in highly metamict zircon and titanite, crystalline nanodomains with original crystallographic orientations might still exist.

In conclusion, Raman spectroscopy, as shown above, is a very powerful tool for study of radiation damage in actinide-bearing phases and for estimation of their long-term durability of their physical properties and chemical stability. This type of Raman applications can provide a better understanding of the mechanism of radiation damage and thermal recrystallization processes. It has a wide usage in condensed mater physics, material science, nuclear material sciences, mineralogist, and geochemistry. It has also been used analysis other radiation-damaged minerals, such as fergusonite [82, 83], actinide-bearing monazite [32], titanoaeschynite (Nd) and

nioboaeschynite (Ce) [84], uranyl titanate mineral davidite-(La) [85], aeschynite-(Y) and polycrase-(Y) [86], and steenstrupine [87], and pyrochlore (Zietlow et al., personal communication).

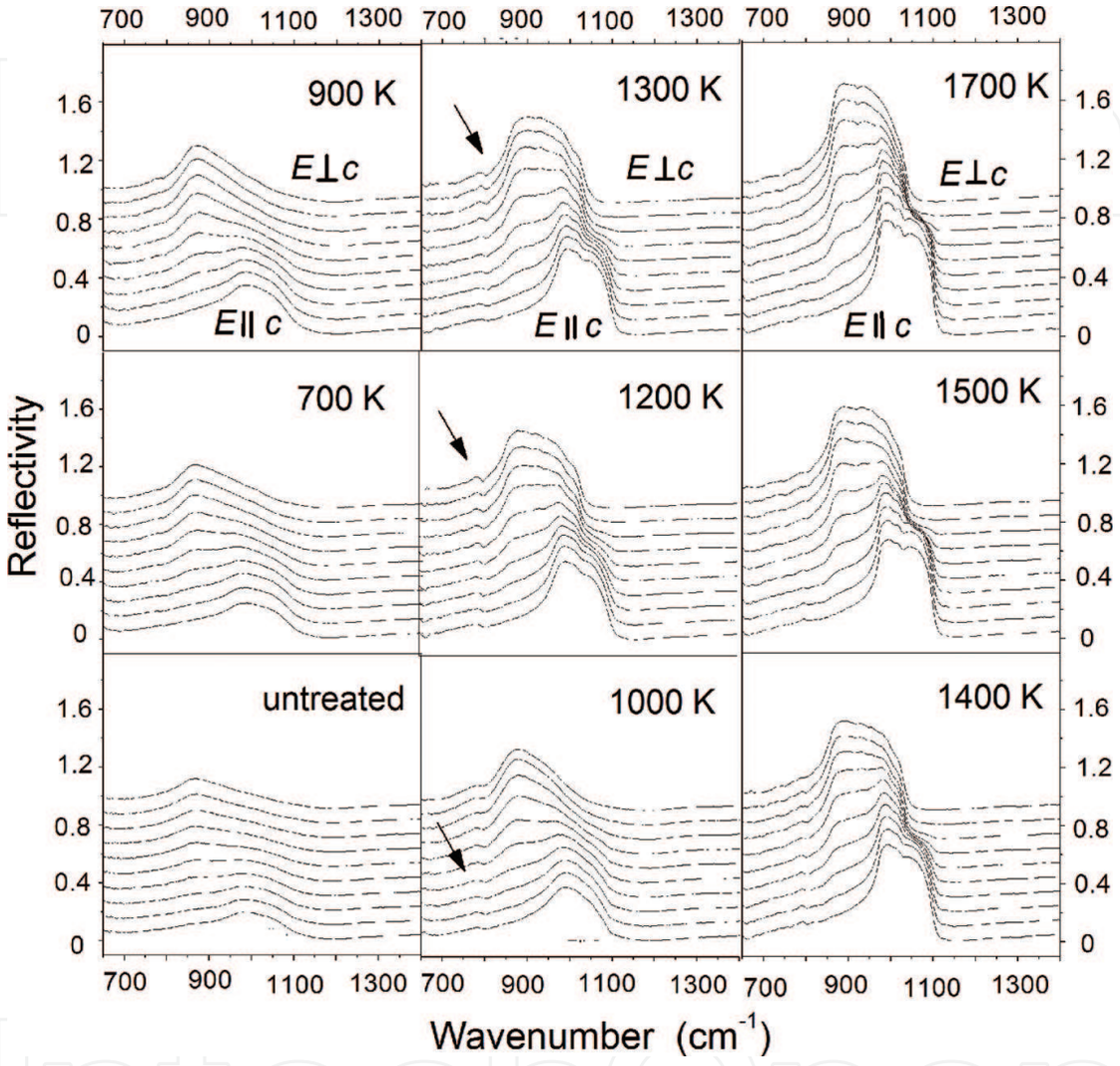

Figure 7. Orientational dependence of polarized infrared spectra of radiation-damaged zircon crystal (dose = 3.8×10^{18} alpha-events g^{-1}) annealed between 292 and 1700 K (Ref. [48], modified). The interval of the angle between the c-axis and the incident radiation E is 10°. The arrows indicate the appearance of an extra signal near 790 cm^{-1}, suggesting a possible intermediate phase. Thermal annealing results in a recovery of the anisotropy of the damage zircon crystal to its original crystallographic orientations.

Author details

Ming Zhang

Address all correspondence to: Ming_zhang@caep.cn

Institute of Materials, China Academy of Engineering Physics, Sichuan, China

References

[1] Ewing RC. Long-term storage of spent nuclear fuel. Nat. Mater. 2015;**14**:252–257.

[2] Ewing RC, Lutze W, Weber WJ. Zircon: a host-phase for the disposal of weapons plutonium. J. Mater. Res. 1995;**10**:243–246.

[3] Weber WJ, Ewing RC, Catlow CRA, de la Rubia TD, Hobbs LW, Kinoshita C, et al. Radiation effects in crystalline ceramics for the immobilization of high-level nuclear waste and plutonium. J. Mater. Res. 1998;**13**:1434–1484. doi:10.1557/JMR.1998.0205

[4] Ewing RC. The design and evaluation of nuclear-waste forms: clues from mineralogy. Can. Mineral. 2001;**39**:697–715. doi:10.2113/gscanmin.39.3.697

[5] Ewing RC. The metamict state: 1993—the centennial. Nucl. Instrum. Methods Phys. Res. Sect. B: Beam Interact. Mater. Atoms 1994;**B91**:22–29. doi:10.1016/0168-583X(94)96186-7

[6] Salje EKH, Chrosch J, Ewing RC. Is "metamictization" of zircon a phase transition? Am. Miner. 1999;**84**:1107–1116.

[7] Ewing RC, Meldrum A, Wang LM, Weber WJ, Corrales LR. Radiation effects in zircon. In Reviews in Mineralogy and Geochemistry, Vol 53, Edited by John Hanchar and Paul Hoskin; published by Mineralogical Society of America and Geochemical Society; 2003. p.387-425.

[8] Zhang M, Salje EKH, Farnan I, Graem-Barber A, Danial P, Ewing RC, Clark AM, Leroux H. Metamictization of zircon: Raman spectroscopic study. J. Phys. Condens. Matter. 2000;**12**:1915. doi:10.1088/0953-8984/12/8/333

[9] Holland HD, Gottfried D. The effect of nuclear radiation on the structure of zircon. Acta Crystallogr. 1955;**8**:291–300. doi:10.1107/S0365110X55000947

[10] Murakami T, Chakoumakos BC, Ewing RC, Lumpkin GR, Weber WJ. Alpha-decay event damage in zircon. Am. Miner. 1991;**76**:1510–1532.

[11] Hawthorne FC, Groat LA, Raudsepp M, Ball NA, Kimata M, Spike FD, Gaba R, Halden NM, Lumpkin GR, Ewing RC, Greegor RB, Lytle FW, Ercit TS, Rossman GR, Wicks FJ, Ramik RA, Sherriff BL, Fleet ME, Mccammon C. Alpha-decay damage in titanite. Am. Miner. 1991;**76**:370–396.

[12] Weber WJ. Alpha-decay-induced amorphization in complex silicate structures. J. Am. Ceram. Soc. 1993;**76**:1729–1738. doi:10.1111/j.1151-2916.1993.tb06641.x

[13] Nasdala L, Zhang M, Kempe U, Panczer G, Gaft M, Andrut M, Plötze M. Spectroscopic methods applied to zircon. Rev. Mineral. Geochem. 2003;**53**:427–467. doi:10.2113/0530427

[14] Zhang M, Salje EKH. Infrared spectroscopic analysis of zircon: radiation damage and the metamict state. J. Phys. Condens. Matter. 2001;**13**:3057–3071. doi:10.1088/0953-8984/13/13/317

[15] Vance ER, Anderson BW. Study of metamict ceylon zircons. Mineral. Mag. 1972;**38**:605–613. doi:10.1180/minmag.1972.038.297.09

[16] Woodhead JA, Rossman GR, Thomas AP. Hydrous species in zircon. Am. Miner. 1991;**76**:1533–1546.

[17] Zhang M, Groat LA, Salje EKH, Beran A. Hydrous species in crystalline and metamict titanites. Am. Miner. 2001;**86**:904–909.

[18] Zhang M, Salje EKH, Ewing RC. OH species, U ions, and CO/CO_2 in thermally annealed metamict zircon ($ZrSiO_4$). Am. Miner. 2010;**95**:1717–1724. doi:10.2138/am.2010.3567

[19] Salje EKH, Zhang M. Hydrous species in ceramics for the encapsulation of nuclear waste: OH in zircon. J. Phys. Condens. Matter. 2006;**18**:L277–L282. doi:10.1088/0953-8984/18/22/L01

[20] Chakoumakos BC, Murakami T, Lumpkin GR, Ewing RC. Alpha-decay-induced fracturing in zircon: the transition from the crystalline to the metamict state. Science (cover). 1987;**236**:1556–1559. doi:10.1126/science.236.4808.1556

[21] Yada K, Tanji T, Sunagawa I. Radiation-induced lattice-defects in natural zircon (zrsio4) observed at atomic resolution. Phys. Chem. Miner. 1987;**14**:197–204.

[22] Wang LM. Application of advanced electron microscopy techniques to the studies of radiation effects in ceramic materials. Nucl. Instrum. Methods Phys. Res. 1998;**B14**1:312–325.

[23] Ewing RC, Haaker RF, Lutze W. Leachability of zircon as a function of alpha dose. In Scientific Basis for Radioactive Waste Management V. Edited by Werner Lutze; Elsevier, Amsterdam, 1982: p. 389–397.

[24] Chakoumakos BC, Oliver WC, Lumpkin GR, Ewing RC. Hardness and elastic-modulus of zircon as a function of heavy-particle irradiation dose. I. *In situ* alpha-decay event damage. Radiat. Eff. Defects Solids. 1991;**118**:393–403. doi:10.1080/10420159108220764

[25] Farnan I. Si-29 NMR characterization of the crystalline-amorphous transition in $ZrSiO_4$. Phase Transitions. 1999;**69**:47–60.

[26] Ríos S, Salje EKH. Diffuse X-ray scattering from weakly metamict zircon. J. Phys. Condens. Matter. 1999;**11**:8947–8956.

[27] Farges F, Calas G. Structural-analysis of radiation-damage in zircon and thorite: an X-ray absorption spectroscopic study. Am. Miner. 1991;**76**:1–2.

[28] Salje EKH, Safarik DJ, Taylor RD, Pasternak MP, Modic KA, Groat LA, Lshley JC. Determination of iron sites and the amount of amorphization in radiation-damaged titanite ($CaSiTiO_5$). J. Phys. Condens. Matter. 2011;**23**:105402. doi:10.1088/0953-8984/23/10/105402

[29] Roberts J, Gaugliardo P, Farnan I, Zhang M, Vance ER, Davis J, et al. Positron annihilation lifetime study of radiation-damaged natural zircons. J. Nucl. Mater. 2016;**471**:44–50. doi:10.1016/j.jnucmat. 2015. 12.008

[30] Zhang M, Salje EKH. Spectroscopic characterization of metamictization and recrystallization in zircon and titanite. Phase Transit. 2003;**76**:117–136. doi:10.1080/0141159031000076093

[31] Nasdala L, Irmer G, Wolf D. The degree of metamictization in zircon: a Raman spectroscopic study. Eur. J. Mineral. 1995;**7**:471–478.

[32] Podor R. Raman spectra of the actinide-bearing monazites. Eur. J. Mineral. 1995;**7**:1353–1360.

[33] Hazen RM, Finger LW. Crystal-structure and compressibility of zircon at high-pressure. Am. Miner. 1979;**64**:196–201.

[34] Dawson P, Hargreave MM, Wilkinson GF. Vibrational spectrum of zircon ($ZrSiO_4$). J. Phys. C Solid State. 1971;**4**:240–256. doi:10.1088/0022-3719/4/2/014

[35] Nasdala L, Pidgeon RT, Wolf D, Irmer G. Metamictization and U-Pb isotopic discordance in single zircons: a combined Raman microprobe and SHRIMP ion probe study. Mineral. Petrol. 1998;**62**:1–27. doi:10.1007/BF01173760

[36] Geisler T, Pidgeon RT, van Bronswijk W, Pleysier R. Kinetics of thermal recovery and recrystallization of partially metamict zircon: a Raman spectroscopic study. Eur. J. Mineral. 2001;**13**:1163–1176. doi:10.1127/0935-1221/2001/0013-1163

[37] Xu XS, Zhang M, Zhu KY, Chen XM, He ZY. Reverse age zonation of zircon formed by metamictisation and hydrothermal fluid leaching. Lithos. 2011;**150**:256–267. doi:10.1016/j.lithos.2011.12.014

[38] Taylor M, Brown GE. High-temperature structural study of the $P2_1$-$A2/a$ phase-transition in synthetic titanite, $CaTiSiO_5$. Am. Miner. 1976;**61**:435–447.

[39] Salje EKH, Schmidt C, Bismayer U. Structural phase transition in titanite, $CaTiSiO_5$: a Raman spectroscopic study. Phys. Chem. Miner. 1993;**19**:502–506.

[40] Zhang M, Salje EKH, Redfern SAT, Bismayer U, Groat LA. Intermediate structures in radiation damaged titanite ($CaTiSiO_5$): a Raman spectroscopic study. J. Phys. Condens. Matter. 2013;**25**:115402. doi:10.1088/0953-8984/25/11/115402

[41] Beirau T, Bismayer U, Mihailova B, Paulmann C, Groat L. Structural phenomena of metamict titanite: a synchrotron, X-ray diffraction and vibrational spectroscopic study. Phase Transit. 2010;**83**:694–702. doi:10.1080/01411594.2010.502875

[42] Salje EKH, Taylor DR, Safarik DJ, Lashley JC, Groat LA, Bismayer U, James ER, Friedman R. Evidence for direct impact damage in metamict titanite $CaTiSiO_5$. J. Phys. Condens. Matter. 2011;**24**:052202. doi:10.1088/0953-8984/24/5/052202

[43] Zhang M, Salje EKH, Bismayer U, Groat L, Malcherek T. Metamictization and recrystallization of titanite: an infrared spectroscopic study. Am. Miner. 2002;**87**:882–890.

[44] Beirau T, Mihailova B, Matveeva G, Kolb U, Malcherek T, Groat LA, Bismayer U. Structural anisotropy and annealing-induced nanoscale atomic rearrangements in metamict titanite. Am. Miner. 2012;**97**:1354–1365. doi:10.2138/am.2012.4024

[45] Beirau T, Mihailova B, Malcherek T, Paulmann C, Groat LA, Bismayer U. Temperature-induced P21/c to c2/c phase transition in partially amorphous (metamict) titanite revealed by Raman spectroscopy. Can. Mineral. 2014;**52**:91–100. doi:10.3749/canmin.52.1.91

[46] Ríos S, Salje EKH, Zhang M, Ewing RC. Amorphization in natural zircon: evidence for direct impact damage. J. Phys. Condens. Matter. 2000;**12**:2401–2412.

[47] Zhang M, Salje EKH, Capitani GC, Leroux H, Clark AM, Schlüter J, Ewing RC. Annealing of alpha-decay damage in zircon: a Raman spectroscopic study. J. Phys. Condens. Matter. 2000;**12**:3131. doi:10.1088/0953-8984/12/13/321

[48] Zhang M, Salje EKH, Ewing RC, Farnan I, Ríos S, Schlüter J, Leggo P. Alpha-decay damage and recrystallization in zircon: evidence for an intermediate state from infrared spectroscopy. J. Phys. Condens. Matter. 2000;**12**:5189. doi:10.1088/0953-8984/12/24/310

[49] Wasilewski PJ, Senftle FE, Vaz JE, Thorpe AN, Alexander CC. A study of the natural a-recoil damage in zircon by infrared spectra. Radiat. Eff. 1973;**17**:191–199.

[50] Farges F. The structure of metamict zircon: a temperature-dependent EXAFS study. Phys. Chem. Miner. 1994;**20**:504–514.

[51] McLaren AC, Fitz JD, Williams IS, McLaren AC, Fitz JD, Williams IS. The microstructure of zircon and its influence on the age determination from Pb/U isotopic ratios measured by ion microprobe. Geochim. Cosmochim. Acta. 1994;**58**:993–1005.

[52] Ellsworth S, Navrotsky A, Ewing RC. Energetics of radiation-damage in natural zircon ($ZrSiO_4$). Phys. Chem. Miner. 1994;**21**:140–149. doi:10.1007/BF00203144

[53] Mursic Z, Vogt T, Frey F. High-temperature neutron powder diffraction study of $ZrSiO_4$ up to 1900 K. Acta Crystallogr. 1992;**B48**:584–590.

[54] Colombo M, Chrosch J. Annealing of natural metamict zircons: II high degree of radiation damage. Radiat. Phys. Chem. 1998;**53**:563–566. doi:10.1016/S0969-806X(98)00194-7

[55] Meldrum A, Zinkle SJ, Boatner LA, Ewing RC. A transient liquid-like phase in the displacement cascades of zircon, hafnon and thorite. Nature. 1998;**395**:56–58. doi:10.1038/25698

[56] Wittels MC, Steigler JO, Sherrill FA. Reactor sciences and technology. J. Nucl. Energy Parts A/B. 1962;**16**:237.

[57] Benyagoub A, Levesque F, Coureur F, Giber-Mougel C, Dufour C, Paumier E. Evidence of a phase transition induced in zirconia by high energy heavy ions. Appl. Phys. Lett. 2000;**77**:3197. doi:10.1063/1.1326483

[58] Smith DK, Newkirk HK. Crystal structure of baddeleyite (monoclinic ZrO_2) and its relation to polymorphism of ZrO_2. Acta Crystallogr. 1965;**18**:983–991. doi:10.1107/S0365110X65002402

[59] Keramidas VG, White WB. Raman-scattering study of crystallization and phase-transformations of ZrO_2. J. Am. Ceram. Soc. 1974;**57**:22–24.

[60] Anastassakis E, Papanicolaou B, Asher IM. Lattice-dynamics and light-scattering in hafnia and zirconia. J. Phys. Chem. Solids. 1975;**36**:667–676. doi:10.1016/0022-3697(75)90085-2

[61] Pavlik RS, Holland HJ, Payzant EA. Thermal decomposition of zircon refractories. J. Am. Ceram. Soc. 2001;**84**:2930–2936.

[62] Váciz T, Nasdala L, Wirth R, Mehofer M, Libowitzky E, Häger T. On the breakdown of zircon upon "dry" thermal annealing. Mineral. Petrol. 2009;**97**:129–138. doi:10.1007/s00710-009-0087-9

[63] Wang AH, Wang WY, Xie CS, Song WL, Zeng DW. CO_2 laser-induced structure changes on a zircon refractory. Appl. Surf. Sci. 2004;**227**:104–113. doi:10.1016/j.apsusc.2003.11.049

[64] Tole MP. The kinetics of dissolution of zircon ($ZrSiO_4$). Geochim. Cosmochim. Acta. 1985;**49**:453–458.

[65] Geisler T, Zhang M, Salje EKH. Recrystallization of almost fully amorphous zircon under hydrothermal conditions: an infrared spectroscopic study. J. Nucl. Mater. 2003;**320**:280–291. doi:10.1016/S0022-3115(03)00187-9

[66] Butterman WC, Foster WR. Zircon stability and ZrO_2-$S10_2$ Phase Diagram. Am. Miner. 1967;**52**:880–885.

[67] Zhang M, Salje EKH, Wang AH, Li XJ, Xie CS, Redfern SAT, Li RX. Vibrational spectroscopy of fast-quenched $ZrSiO_4$ melts produced by laser treatments: local structures and decomposed phases. J. Phys. Condens. Matter. 2005;**17**:6363–6376. doi:10.1088/0953-8984/17/41/007

[68] Zhang M, Ewing RC, Boatner LA, Salje EKH, Weber WJ, Daniel P, Zhang Y, Farnan I. Pb^+ irradiation of synthetic zircon ($ZrSiO_4$): infrared spectroscopic investigation—reply. Am. Mineral. 2009;**94**:856–858.

[69] Sales BC, Ramey JO, Boatner LA, McCallum JC. Structural inequivalence of the ion-damage-produced amorphous state and the glass state in lead pyrophosphate. Phys. Rev. Lett. 1989;**62**:1138–1141. doi:10.1103/PhysRevLett.62.1138

[70] Zhang M, Boatner L, Salje EKH, Ewing RC, Daniel P, Weber WJ, Zhang Y, Farnan I. Micro-Raman and micro-infrared spectroscopic studies of Pb- and Au-irradiated $ZrSiO_4$: optical properties, structural damage, and amorphization. Phys. Rev. B. 2008;**77**:144110. doi:10.1103/PhysRevB.77.144110

[71] Magruder RH, Morgan SH, Weeks RA, Zuhr RA. Effects of ion implantation on intermediate range order: IR spectra of silica. J. Non-Cryst. Solids. 1990;**120**:241–249.

[72] Magruder RH, Henderson DO, Morgan SH, Zuhr RA. Optical-spectra of pb implanted fused-silica. J. Non-Cryst. Solids. 1993;**152**:258–266. doi:10.1016/0022-3093(93)90259-Z

[73] Arnold GW, Brow RK, Myers DR. Characterization of the near-surface region of glass implanted with light elements. J. Non-Cryst. Solids. 1990;**120**:234–240.

[74] Arnold GW. Ion-implantation effects in glasses. Radiat. Eff. Defects Solids. 1998;**65**:17–30. doi:10.1080/00337578208216813

[75] Capitani GC, Leroux H, Doukhan JC, Ríos S, Zhang M, Salje EKH. A TEM investigation of natural metamict zircons: structure and recovery of amorphous domains. Phys. Chem. Miner. 2000;**27**:545–556. doi:10.1007/s002690000100

[76] Vance ER. Alpha-recoil damage in zircon. Radiat. Eff. 1975;**24**:1–6. doi:10.1080/00337577508239470

[77] Zhang M, Salje EKH, Ewing RC. Oxidation state of uranium in metamict and annealed zircon: near infrared spectroscopic quantitative analysis. J. Phys. Condens. Matter. 2003;**15**:3445–3470

[78] Weber WJ. Self-radiation damage and recovery in pu-doped zircon. Radiat. Eff. Defects Solids. 1991;**115**:341–349. doi:10.1080/10420159108220580

[79] Lumpkin GR, Foltyn EM, Ewing RC. Thermalrecrystallization of alpha-recoil damaged minerals of thepyrochlore structure type. J. Nucl. Mater. 1986;**139**:113. doi:10.1016/0022-3115(86)90029-2

[80] Chrosch J, Colombo M, Malcherek T, Salje EK, Groat LA, Bismayer U. Thermal annealing of radiation damaged titanite. Am. Miner. 1998;**83**:1083–1091.

[81] Nasdala L, Beran A, Libowitzky E, Wolf D. The incorporation of hydroxyl groups and molecular water in natural zircon ($ZrSiO_4$). Am. J. Sci. 2001;**301**:831–857. doi:10.2475/ajs.301.10.831

[82] Tomašić N, Gajović A, Bermanec V, Su DS, Rajić Linarić M, Ntaflos T, Schlögl R. Recrystallization mechanisms of fergusonite from metamict mineral precursors. Phys. Chem. Miner. 2006;**33**:145–159. doi:10.1007/s00269-006-0061-6

[83] Ruschel K, Nasdala L, Rhede D, Wirth R, Lengauer CL, Libowitzky E. Chemical alteration patterns in metamict fergusonite. Eur. J. Mineral. 2010;**22**:425–433. doi:10.1127/0935-1221/2010/0022-2031

[84] Xue LH, Gong W. A study on Raman and photoluminescence spectra of the aeschynite group minerals. J. Non-Cryst. Solids. 2000;**20**:827–829.

[85] Frost RL, Reddya BJ. The effect of metamictization on the Raman spectroscopy of the uranyl titanate mineral davidite (La,Ce)(Y,U,Fe^{2+})(Ti,Fe^{3+})(20)(O,OH)(38). Radiat. Eff. Defects Solids. 2011;**166**:131–136. doi:10.1080/10420150.2010.516394

[86] Tomašić N, Gajović A, Bermanec V, Rajić M. Recrystallization of metamict Nb-Ta-Ti-REE complex oxides: a coupled X-ray-diffraction and Raman spectroscopy study of aeschynite-(Y) and polycrase-(Y). Can. Mineral. 2004;**42**:1847–1857. doi:10.2113/gscanmin.42.6.1847

[87] Kusz J, Malczewski D, Zubko M, Häger T,Hofmeister T.High temperature study of metamict steenstrupine. Solid State Phenomena, 2010, 163:253-255